AD-A061 747   TEXAS UNIV AT AUSTIN DEPT OF CHEMISTRY   F/G 9/1
SEMICONDUCTOR ELECTRODES. 19. AN INVESTIGATION OF S/SE SUBSTITU--ETC(U)
NOV 78   R N NOUFI, P A KOHL, J W ROGERS   N00014-75-C-0922

UNCLASSIFIED   NL

1 OF 1
ADA
061747

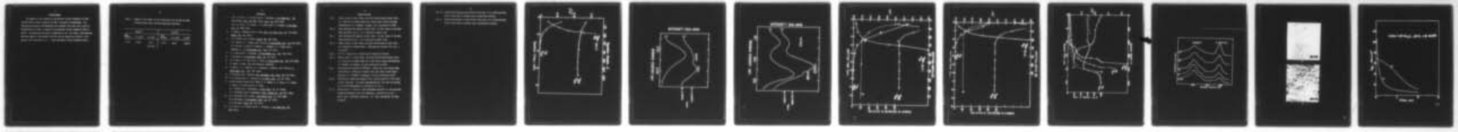

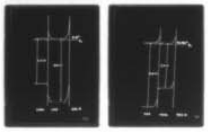

END
DATE
FILMED
2-79
DDC

12

OFFICE OF NAVAL RESEARCH

Contract No. N00014-75-C-0922

Task No. NR 056-578

Technical Report No. 7

Semiconductor Electrodes. 19. An Investigation of S/Se Substitution in Single Crystal CdSe and CdS Photoelectrodes by Electron Spectroscopy.

by

Rommel N. Noufi, Paul A. Kohl, James W. Rogers, Jr.,
John M. White and Allen J. Bard

Prepared for Publication
in
Journal of Electrochemical Society

Department of Chemistry
University of Texas at Austin
Austin, Texas 78712

November 1, 1978

SECURITY CLASSIFICATION OF THIS PAGE *(When Data Entered)*

REPORT DOCUMENTATION PAGE

READ INSTRUCTIONS
BEFORE COMPLETING FORM

1. REPORT NUMBER

2. GOVT ACCESSION NO.

3. RECIPIENT'S CATALOG NUMBER
(9)

4. TITLE *(and Subtitle)*
(6) Semiconductor Electrodes. 19. An Investigation of S/Se Substitution in Single Crystal CdSe and CdS Photoelectrodes by Electron Spectroscopy.

~~5. TYPE OF REPORT & PERIOD COVERED~~
Technical Report. no. 1
~~January 1, 1978-Dec. 31, 1978~~

~~6. PERFORMING ORG. REPORT NUMBER~~
1 Jan - 31 Dec 78,

7. AUTHOR(s)
(10) Rommel N./Noufi, Paul A./Kohl, James W./Rogers, Jr, John M./White ~~and~~ Allen J./Bard

~~8. CONTRACT OR GRANT NUMBER(s)~~
(15) N00014-75-C-0922

9. PERFORMING ORGANIZATION NAME AND ADDRESS
J. M. White, Department of Chemistry
University of Texas at Austin
Austin, Texas 78712

10. PROGRAM ELEMENT, PROJECT, TASK AREA & WORK UNIT NUMBERS
Project NR 056-578

11. CONTROLLING OFFICE NAME AND ADDRESS
Department of the Navy
Office of Naval Research
Arlington, Virginia 22217

12. REPORT DATE
(11) 1 Nov~~ember 1~~, 1978

13. NUMBER OF PAGES
26

14. MONITORING AGENCY NAME & ADDRESS *(if different from Controlling Office)*
(12) 28p.

15. SECURITY CLASS. *(of this report)*

15a. DECLASSIFICATION/DOWNGRADING SCHEDULE

16. DISTRIBUTION STATEMENT *(of this Report)*

Approved for Public Release: Distribution Unlimited

17. DISTRIBUTION STATEMENT *(of the abstract entered in Block 20, if different from Report)*

18. SUPPLEMENTARY NOTES

Preprint, to be submitted to Journal of Electrochemical Society

19. KEY WORDS *(Continue on reverse side if necessary and identify by block number)*

20. ABSTRACT *(Continue on reverse side if necessary and identify by block number)*

Photoelectron spectroscopy studies verify the occurrence of S/Se substitution in single crystal CdSe and CdS photoanodes when used in photoelectrochemical cells containing $S_{\downarrow}^{2-}$ or $Se_{\downarrow}^{2-}$ solutions. A possible mechanism of the S/Se exchange is discussed as well as its consequences on the electrode stability and the output parameters of the photoelectrochemical cells.

78 11 28 031

DD FORM 1 JAN 73 1473 EDITION OF 1 NOV 65 IS OBSOLETE
S/N 0102-014-6601

LB

347 830

SECURITY CLASSIFICATION OF THIS PAGE *(When Data Entered)*

Semiconductor Electrodes. 19. An Investigation of S/Se Substitution in Single Crystal CdSe and CdS Photoelectrodes by Electron Spectroscopy.

Rommel N. Noufi,* Paul A. Kohl,* James W. Rogers, Jr.,
John M. White and Allen J. Bard**
Department of Chemistry
The University of Texas at Austin
Austin, Texas 78712

*ECS Student Member

**ECS Active Member

Key words: ESCA, Energy Conversion, Photoelectricity.

(ABSTRACT)

Photoelectron spectroscopy studies verify the occurrence of S/Se substitution in single crystal CdSe and CdS photoanodes when used in photoelectrochemical cells containing S^{2-} or Se^{2-} solutions. A possible mechanism of the S/Se exchange is discussed as well as its consequences on the electrode stability and the output parameters of the photoelectrochemical cells.

(End of Abstract)

INTRODUCTION

A number of studies have shown that cadmium chalcogenide photoelectrodes can be stabilized in aqueous soluitons by the addition of sulfide, selenide, or telluride ions [1-3]. This stabilization is attributed to the favorable redox potential of the X/X^{2-} couple (X = S, Se, Te) [4,5] compared to the potential where electrode oxidation can occur or the preferential adsorption of sulfide ions for the case of CdS. Recently [6], the behavior of mixed CdS/CdSe solid solution photoelectrodes in polysulfide soluitons was described, where changes in the flat band potential and band-gap with variations in the S/Se ratio were observed.

Although CdS and CdSe show quite stable operation in sulfide and selenide electrolytes, changes in the photocurrent with time are observed and indeed one would expect from thermodynamic reasoning that exchange of solution chalcogenide ions with semiconductor lattice ions would occur. Recent reports [7-9] indeed have provided evidence for such substitution. Thus Hodes _et al_. [7] showed by x-ray photoelectron spectroscopy (XPS or ESCA) that sulfide substitution occurs on polycrystalline CdSe. Similarly Heller _et al_. [8] found evidence of S-substitution in CdSe by Auger electron spectroscopy (AES) and electron beam luminescence. Gerischer and Gobrecht [9] also proposed that changes occur in the surface of CdS and CdSe single crystals under illumination in sulfide electrolytes based upon changes in the photocurrent spectra and Mott-Schottky plots with operation time.

We report here detailed AES and XPS studies of the surface changes which occur in single crystal CdS and CdSe photoanodes when used in photoelectrochemical cells (PEC). The results show that Se substitution occurs in the CdS/Se^{2-} system and S substitution occurs in the CdSe/S^{2-} system and provide information about the mechanism of stabilization and its effect on the output parameters of the PEC.

EXPERIMENTAL

The electrochemical cells, light sources, method of electrode preparation and instrumentation were the same as those previously described [6]. Both single crystals (Cleveland Crystals, Cleveland, Ohio) and the polycrystalline powder (Ventron, Beverly, Mass.) were of high purity (99.999+%). We showed that the CdS was Se-free and the CdSe was S-free, as specified by the manufacturers, by AES and XPS analysis. Surface treatment carried out prior to use involved polishing of the single crystals with 6 μm alumina to a mirror finish followed by a chemical etch. The CdS crystals were etched in 6 M HCl for 30 seconds followed by rinsing with deionized water, while the CdSe crystals were etched for 30 seconds in concentrated HNO_3 followed by rinsing with a 0.1 M KCN solution to dissolve any Se formed during etching, then followed by rinsing with deionized water. Na_2S and Na_2Se solutions were prepared from analytical grade reagents. The Na_2Se solutions were obtained by bubbling H_2Se into a 1 M NaOH solution under nitrogen. The Na_2S solution was filtered twice then deaerated and stored under nitrogen. All experiments were performed under positive nitrogen pressure. Stirring was accomplished with a magnetic stirrer. After performing the photoelectrochemical experiments, the electrodes were rinsed with 1 M Na_2S solution followed by copious amounts of deaerated deionized water.

PEC experiments were run with the electrodes potentiostated at -0.5 V vs. SCE using a large Pt counterelectrode (~ 10 cm^2). The photocurrents produced under illumination with white light (intensities of 20-180 mW/cm^2) were 2-43 ma/cm^2. The electrodes were employed as photoanodes for different amounts of photocharge passing through the electrode surface and compared to electrodes that were immersed at open circuit in the appropriate solution.

Thin films (~500 Å) of both CdSe and CdS on platinum foils (1.5 x 1.5 cm) were prepared by vacuum evaporation of the powders from a hot tungsten filament. The film thickness was determined with a Sloan Model 200 Thickness Monitor (Santa Barbara, Calif.). These films were used to calibrate the sputtering rate of CdS and CdSe by the argon ion beam in the electron spectroscopy analysis.

AES and XPS analysis were performed with a Physical Electronics Model 548 Spectrometer (Eden Prairie, Minn.). A 5 kV, 10-15 μA, focused electron beam was used to excite the substrate during AES measurements. While depth profiling, the voltage ramp was multiplexed such that the S(LMM) (152eV), C(KLL) (272eV), Cd(MNN) (376eV), and Se(LMM) (1315eV) transitions could be sequentially scanned in less than 1 minute. The argon ion beam used for sputter etching was operated at 5 kV and 30 ma emission yielding a uniform beam with a current density of 3.55 $\mu A/cm^2$. The cross sectional area of the circular sputtered crater was approximately 0.13 cm^2. XPS measurements were taken utilizing both Al Kα and Mg Kα anodes. The data were collected digitally using pulse counting and signal averaging techniques. Both broad scan 0-100 eV binding energy (resolution = 1.6 eV FWHM) and high resolution (0.8 eV FWHM) XPS analysis were carried out on the samples as a function of sputter time. During the sputtering process the ion pump was turned off and the vacuum chamber backfilled to 1×10^{-5} torr in Ar. While making XPS measurements the background pressure was maintained in the 5×10^{-9} - 5×10^{-8} torr range. Residual gas analysis showed the major contaminants to be H_2O and CO at these pressures. The intensity of a XPS transition is proportional to the peak area and can be expressed as

$$I = I_0 \, n \, \sigma \, \lambda(\epsilon) \, D(\epsilon)$$

where I_0 = x-ray flux, n = atomic density, σ = cross section for ionization, $\lambda(\epsilon)$ = mean free path of the escaping electron, and $D(\epsilon)$ = the detector efficiency. The ratio of intensities for two elements can then be expressed [10] as

$$\frac{I_a}{I_b} = \frac{n_a}{n_b}\left(\frac{\sigma_a\lambda_a D_a}{\sigma_b\lambda_b D_b}\right) = \frac{n_a}{n_b}\,(Y)$$

The expression in parenthesis remains constant to a first approximation for a given matrix and thus can be determined empirically from standard samples. Both high purity pressed powders and clean single crystals were used to determine Y. Ratios of atomic densities could then be derived from intensity ratios. Using the same standards, relative Auger sensitivities were determined from peak-to-peak height ratios.

Sputtering rates were calibrated by depth profiling CdS and CdSe films of known thickness. The Cd (376 eV), S (152 ev), and Pt (237 eV) peaks were monitored while sputtering; the sputtering process was judged complete when the Cd and S signals were reduced to the noise level. Two profiles were run on each film, the craters being well isolated on opposite sides of the film as judged visually by the bright, shiny platinum at the crater bottom. By this method, sputtering rates for CdS and CdSe of 16±3 and 19±3 Å/min, respectively were found. This corresponds to a sputtering efficiency of 2.4 molecules/ion for CdS and 2.6 molecules/ion for CdSe. A constant Cd/Se Auger peak-to-peak height ratio during the sputtering process indicated that Cd and Se were removed from the surface region at the same rate. Overlap of a platinum transition with the S (152 eV) peak precluded any such determination on CdS. The fact that the CdS and CdSe sputtering rates are the same within experimental error indicates that preferential sputtering is not significant.

RESULTS

CdSe single crystals. - Three CdSe single crystals were examined by electron spectroscopy after various pre-treatments. One crystal was soaked in 1 M NaOH, 1 M Na_2S, 1 M S, solution for 30 min. at open circuit under illumination; the other two crystals were used as photoanodes in a PEC with a total charge passed of 2.5 C/cm^2 and 12.0 C/cm^2 in a similar solution. Initial AES and XPS analysis after immersion and transfer to the spectrometer showed large amounts of C with lesser amounts of O on all of the crystals. The open circuit crystal showed a small amount of S on the surface which was completely removed with less than one minute of Ar^+ bombardment. The C signal was also reduced to its background level with this same amount of sputtering. Whether this S is substituted, as suggested by Heller and Miller et al. [8] or merely adsorbed on the surface cannot be ascertained from our data but it is evident that S is only present in the first few atomic layers. A large amount of S was found in the surface region on the crystal which had been anodized for 2.5 C/cm^2. The ratios of AES peak-to-peak heights for Cd/Se, S/Cd, and Se/S as a function of sputter depth given in Fig. 1, suggest that sulfur is substituted to a depth of 40 Å which corresponds to about 12 atomic layers. The high resolution XPS spectra of the S (2s) - Se (3s) and S (2p) - Se (3p) regions after 0.5 and 8 min. of sputtering are given in Figs. 2 and 3. Contributions from both Se and S are evident after 0.5 min. of sputtering but the S signal is completely gone after 8 min. The C signal on this sample was reduced to its background level by less than one min. of sputtering. The CdSe crystal which was anodized for 12 C/cm^2 showed S substitution to a depth of about 67 Å or 20 atomic layers as shown by the atomic ratios of S/Cd, Cd/Se, and Se/S vs. sputter depth for this crystal (Fig. 4). The solid lines are from AES peak-to-peak height ratios corrected for elemental sensitivity as determined from the standard samples. In addition to the crystal which was anodized for 12 C/cm^2 in 1 M Na_2S, another CdSe crystal was anodized under the same conditions except the solution was also 0.05 M in dissolved Se. This has been shown to decrease the rate of current decay of CdSe photoanodes in S^{2-} media under extended electrolysis [8]. A plot of the AES results for this anode in Fig. 5 (compared to Fig. 4) indicates S substitution to a depth of 33 Å. Besides the usual contaminants of C and O, traces of Na and SiO_2 were initially present on the surface of this crystal. The Na probably arises from the Na_2S solution itself and the trace of SiO_2 could originate from the silicone rubber sealant used to isolate the rear portions of the crystal from the solution, or from attack of the alkaline solutions on the Pyrex cells.

CdS. - CdS single crystals were pretreated in a manner similar to the CdSe crystals. One was immersed at open circuit for 30 min. in 1 M NaOH, 0.5 M Na_2Se, 0.5 M Se solution while two others were anodized in a similar solution for times equivalent to 0.5 C/cm^2 and 6 C/cm^2. Again C and O were initially observed on the surface of all of these crystals. The small amount of Se initially present on the open circuit sample again was removed in less than one minute of sputtering indicating no Se substitution beyond the surface region. The crystal which had been anodized for 0.5 C/cm^2 showed a layer of pure Se 250 Å deep, followed by a region of Se substitution into the CdS about 240 Å in depth.

This Se overlayer was highly contaminated with C as seen from Fig. 6. The C was essentially reduced to its background level as the region of substitution was approached. We define the region of substitutuion in this crystal to begin where the Cd and S signals first appear. The S (2p) - Se (3p) and Se x-ray induced regions as a function of sputter time for the 6 C/cm^2 crystal is shown in Fig. 7.

The Se x-ray induced Auger transition, which appears at a binding energy of 178 eV when an Al Kα anode is used for excitation, is also shown. Even after this sample was sputtered for a total of 51 minutes Se could still be detected, as shown in Fig. 7. This indicates that Se substitutuion occurs deep into the bulk, greater than 800 Å in this case. The results on both CdSe and CdS crystals are summarized in Table 1.

DISCUSSION

It is clear from the results that S/Se substitution takes place in both systems, i.e., from a polysulfide solution into the CdSe photoanode and from the polyselenide solution into the CdS photoanode. The extent of substitution of Se into CdS is greater than S into CdSe, as indicated by the relative depth of penetration. The solubility product constants for CdS and CdSe are 5×10^{-28} and 1×10^{-31}, respectively, as calculated from thermodynamic data [11]. That the substitution of the anion is greatly enchanced upon the passage of charge under illumination is clear from the data given in Table 1. The exchange could occur via some initial photo-oxidation of the CdS and CdSe electrodes in a manner suggested by several investigators [4, 12], followed by reprecipitation of the Cd^{2+}:

$$\underline{CdSe} + 2p^{+} \longrightarrow Cd^{2+} + \underline{Se} \qquad (1)$$

$$\underline{Se} + S^{2-} \longrightarrow SSe^{2-} \qquad (2)$$

$$Cd^{2+} + S^{2-} \longrightarrow \underline{CdS} \qquad (3)$$

and

$$\underline{CdS} + 2p^{+} \longrightarrow Cd^{2+} + \underline{S} \qquad (4)$$

$$\underline{S} + Se^{2-} \longrightarrow SSe^{2-} \qquad (5)$$

$$Cd^{2+} + Se^{2-} \longrightarrow \underline{CdSe} \qquad (6)$$

Because of the high concentration of the anion in solution the Cd^{2+} will precipitate very quickly as CdS or CdSe. The pure Se layer found in one of the CdS samples can probably be attributed to slow kinetics in (2), as also found by Wrighton et al. [13]. The newly formed material will probably possess a more polycrystalline character of different composition, as suggested by Gerischer and Gobrecht [9]. A 600-magnification SEM picture (Fig. 8) clearly shows the change in the surface nature of a CdS electrode before and after anodization in a polyselenide solution. The increased roughness and graininess of the surface probably indicates a regenerated one by the reprecipitation of CdSe to give a surface containing both anions and exhibiting a polycrystalline character with a different doping level, resistivity, adsorption characteristics toward the anions in solution, and electron affinity. We have recently described the behavior of CdS-CdSe solid solution electrodes [6] and showed that the flat band potential and open circiut voltage changed with electrode composition. We attributed this behavior to a change in the electron affinity with the change in composition of the anions. Just as the open circuit voltage (V_{oc}) increased with the above solid solution electrodes as the composition of one of the anions was increased, a similar change in the V_{oc} was observed with the CdS and CdSe photoanodes as the anion substitution proceeded.

The short circuit current of these electrodes has been shown by several groups [7,8], and was confirmed in this laboratory, to decrease with operation time. The rate of the initial decrease was greater for higher intensities (routinely, initial currents of 5 to 40 ma/cm^2 corresponding to 50 to 180 mW/cm^2 white light intensities). Typical behavior of the photocurrent for a CdSe operated in a polysulfide solution is shown in Fig. 9. This deactivation can be rationalized in terms of the energy level diagram one can establish for these substituted electrodes. If the operation of these electrodes is carried long enough so that a substituted layer is formed at the surface of the electrode, the energy level diagram for equilibrium condition will be as shown in Fig. 10 for a CdS layer on CdSe electrode and in Fig. 11 for CdSe on CdS. The relative position of the conduction bands for both materials was taken from the electron affinities. From Fig. 10 one sees that a layer of larger band gap n-type semiconductor on a similar semiconductor of smaller band gap will tend to inhibit the passage of holes to the surface and the flow of electrons into the bulk. In the opposite situation, i.e., a CdSe layer on a CdS electrode, the flow of holes to the surface is favorable, however the flow of electrons into the bulk is inhibited as seen in Fig. 11. The magnitude of the barrier is progressively changing as X changes in the $CdSe_{1-X} S_X$ and $CdS_{1-X} Se_X$ with operation time. $X = 1$ means formation of a substituted layer. Other factors to be considered are a lattice mismatch between CdS and CdSe, and the possibility of defects at the surface of the newly formed layer which creates traps and thus sites for carrier recombination.

Recently, Heller and Miller and co-workers [8] showed that the current blockage in a CdSe electrode can be reduced or eliminated by maintaining an adequate amount of dissolved selenium in the polysulfide solution which resulted in maintaining adequate selenium concentration in the surface film. In this work the results as shown in Fig. 5 indicate that substitution of S for Se into a CdSe electrode operated in a selenium containing polysulfide solution is appreciably reduced.

In summary, we show in this work that although CdS and CdSe are stable against photodissolution in polysulfide and polyselenide solutions, the latter contribute, through anion substitution, to the deterioration of the output parameters, with time of operation.

ACKNOWLEDGMENT

The support of this research by the National Science Foundation (to AJB) and the Office of Naval Research (to JMW) is gratefully acknowledged. The electron spectroscopy instrumentation was purchased from funds from a grant to The University of Texas at Austin by the National Science Foundation (CHE 76-05172). We appreciate the helpful suggestions of Drs. Gary Hodes, Joost Manassen, and David Cahen of the Weizmann Institute and the cooperative efforts of this group in this area under a U.S. - Israel Binational Science Foundation grant.

Table 1. Summary of the extent of S/Se substitution for the CdS and CdSe photoelectrodes under different operating conditions.

$CdSe/S^{2-}$			CdS/Se^{2-}		
Open Circuit	2.5 C/cm^2	12 C/cm^2	Open Circuit	0.5 C/cm^2	6 C/cm^2
< 12 Å	∿ 40 Å	67 Å (33 Å-Se)	< 12 Å	240 Å	> 800 Å

REFERENCES

1. a) A. B. Ellis, S. W. Kaiser and M. S. Wrighton, J. Am. Chem. Soc., 98, 1635 (1976); ibid., 98, 6855 (1976); ibid., 98, 6418 (1976).

   b) A. B. Ellis, S. W. Kaiser, J. M. Bolts and M. S. Wrighton, J. Am. Chem. Soc., 99, 2839 (1977).

2. G. Hodes, J. Manassen, and D. Cahen, Bull. Isr. Phys. Soc., 22, 100 (1976); Nature, 261, 403 (1976).

3. a) B. Miller, and A. Heller, Nature, 262, 680 (1976).

   b) A. Heller, K. C. Chang, and B. Miller, J. Electrochem. Soc., 124, 697 (1977).

   c) B. Miller, A. Heller, M. Robbins, S. Menezes, K. C. Chang, and J. Thompson, Jr., J. Electrochem. Soc., 124, 1019 (1977).

4. A. J. Bard and M. S. Wrighton, J. Electrochem. Soc., 124, 1706 (1977).

5. H. Gerischer, J. Electroanal. Chem., 82, 133 (1977).

6. R. N. Noufi, P. A. Kohl and A. J. Bard, J. Electrochem. Soc., 125, 375 (1978).

7. D. Cahen, G. Hodes, and Joost Manassen, submitted.

8. A. Heller, J. P. Schwartz, A. G. Vadimsky, S. Menezes, and B. Miller, J. Electrochem. Soc., 125, 1156 (1978).

9. H. Gerischer and J. Gobrecht, Ber. Bunsenges. Phys. Chem., 82, 520 (1978).

10. R. B. Shalvoy and P. J. Reucroft, J. of Elect. Spec., 12, 351 (1977).

11. a) NBS Technical Note 270-3 (1968), D. D. Wagman, W. H. Evans, V. B. Parker, I. Halow, S. M. Bailey and R. H. Schum.

    b) J. Drowarf and P. Goldfinger, J. Chim. Phys., 55, 721 (1958).

    c) P. Goldfinger and M. Jeunehomme, Trans. Faraday Soc., 59, 2851 (1963).

12. a) H. Gerischer and W. Minalt, Electrochim. Acta, 13, 1239 (1968).

    b) H. Gerischer, J. Electroanal. Chem., 58, 263 (1975).

    c) H. Gerischer, ibid., 82, 133 (1977).

13. A. B. Ellis, S. W. Kaiser, and M. S. Wrighton, J. Am. Chem. Soc., 98, 6855 (1976).

FIGURE CAPTIONS

Fig. 1 Atomic ratios of Se/S, Cd/Se, and S/Cd from AES peak-to-peak ratios as a function of sputter depth for a CdSe single crystal electrode photoanodized in a 1 M NaOH, 1 M Na_2S, 1 M S solution, (2.5 C/cm^2).

Fig. 2 High resolution XPS spectra of the S (2s) - Se (3s) region of the same CdSe electrode in Fig. 1 as a function of sputter time.

Fig. 3 High resolution XPS spectra of the S (2p) - Se (3p) region of the same CdSe electrode in Fig. 1 as a function of sputter time.

Fig. 4 Atomic ratios of Se/S, Cd/Se, and S/Cd from AES peak to peak ratios as a function of sputter depth. Electrode and solution as in Fig. 1, (12 C/cm^2).

Fig. 5 As Fig. 4 except for a solution also containing 0.05 M Se.

Fig. 6 Atomic ratios of S/Se, Cd/Se, and S/Cd from AES peak-to-peak ratios as a function of sputter depth for a CdS single crystal photoanodized in 1 M NaOH, 0.5 M Na_2Se, 0.5 M Se solution, (0.5 C/cm^2).

Fig. 7 High resolution spectra of the S(2p) - Se(3p) and x-ray induced Auger transition as a function of sputter time. CdS single crystal photoanodized in a 1 M NaOH, 0.5 M Na_2Se, 0.5 M Se solution, (6 C/cm^2).

Fig. 8 SEM pictures showing the change in the surface nature of a CdS single crystal electrode: (a) before photoanodization; (b) after the passage of 0.2 C/cm^2 photocharge in a solution as in Fig. 7.

Fig. 9 Photocurrent vs. time for a CdSe photoanode operated in a two electrode photoelectrochemical solar cell employing a solution as in Fig. 1. White light illumination intensity: (a) about 180 mW/cm^2; (b) about 50 mW/cm^2.

Fig. 10 Energy band diagram, at equilibrium in the dark, of a n-CdSe electrode with a n-CdS layer in contact with a polysulfide solution.

Fig. 11 Energy band diagram, at equilibrium in the dark, of a n-CdS electrode with a n-CdSe layer in contact with a polyselenide solution.

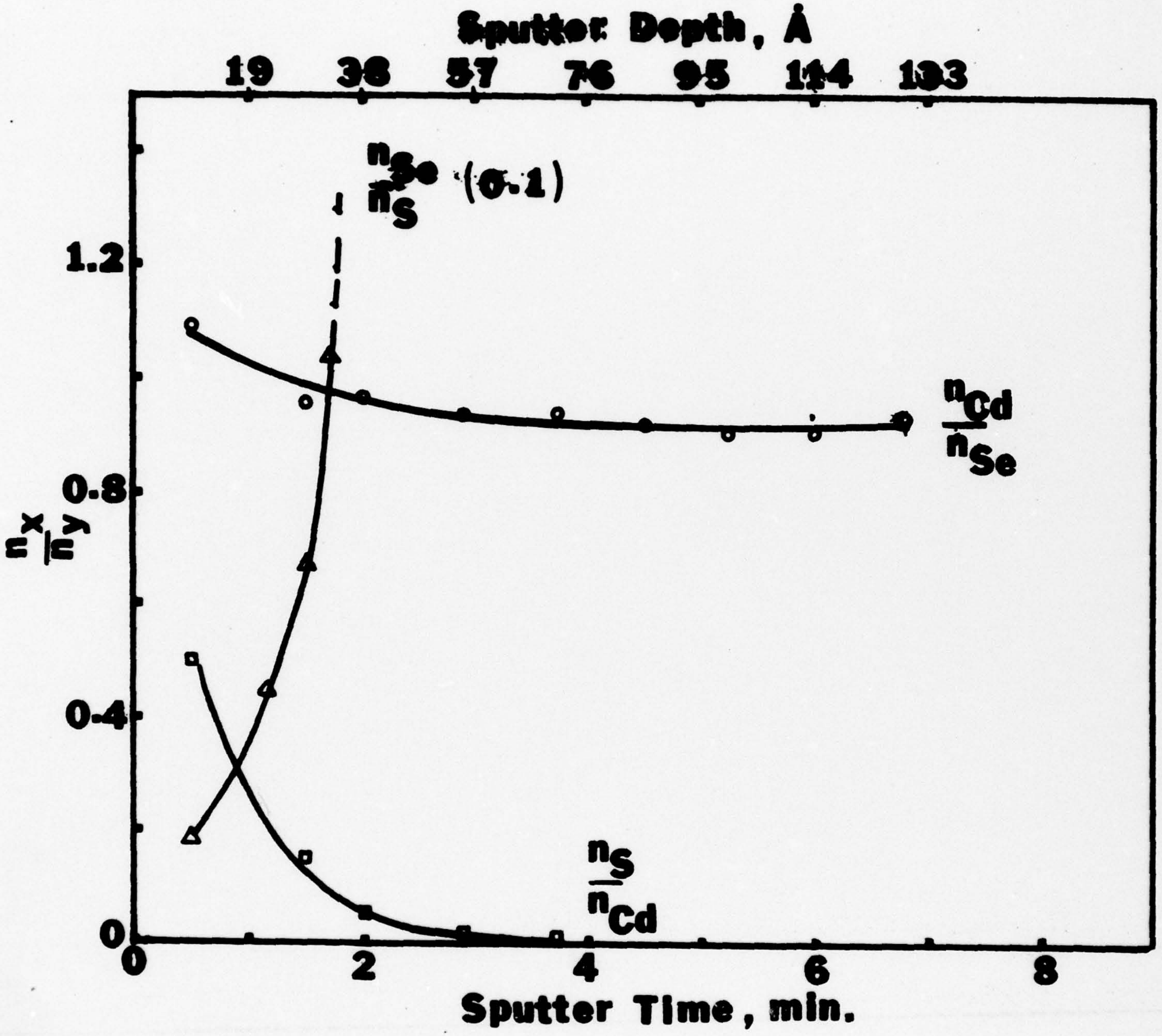
Sputter Depth, Å
19
38
57
76
95
114
133
n_{Se}/n_S (σ·1)
n_{Cd}/n_{Se}
n_S/n_{Cd}
n_x/n_y
1.2
0.8
0.4
0
0
2
4
6
8
Sputter Time, min.

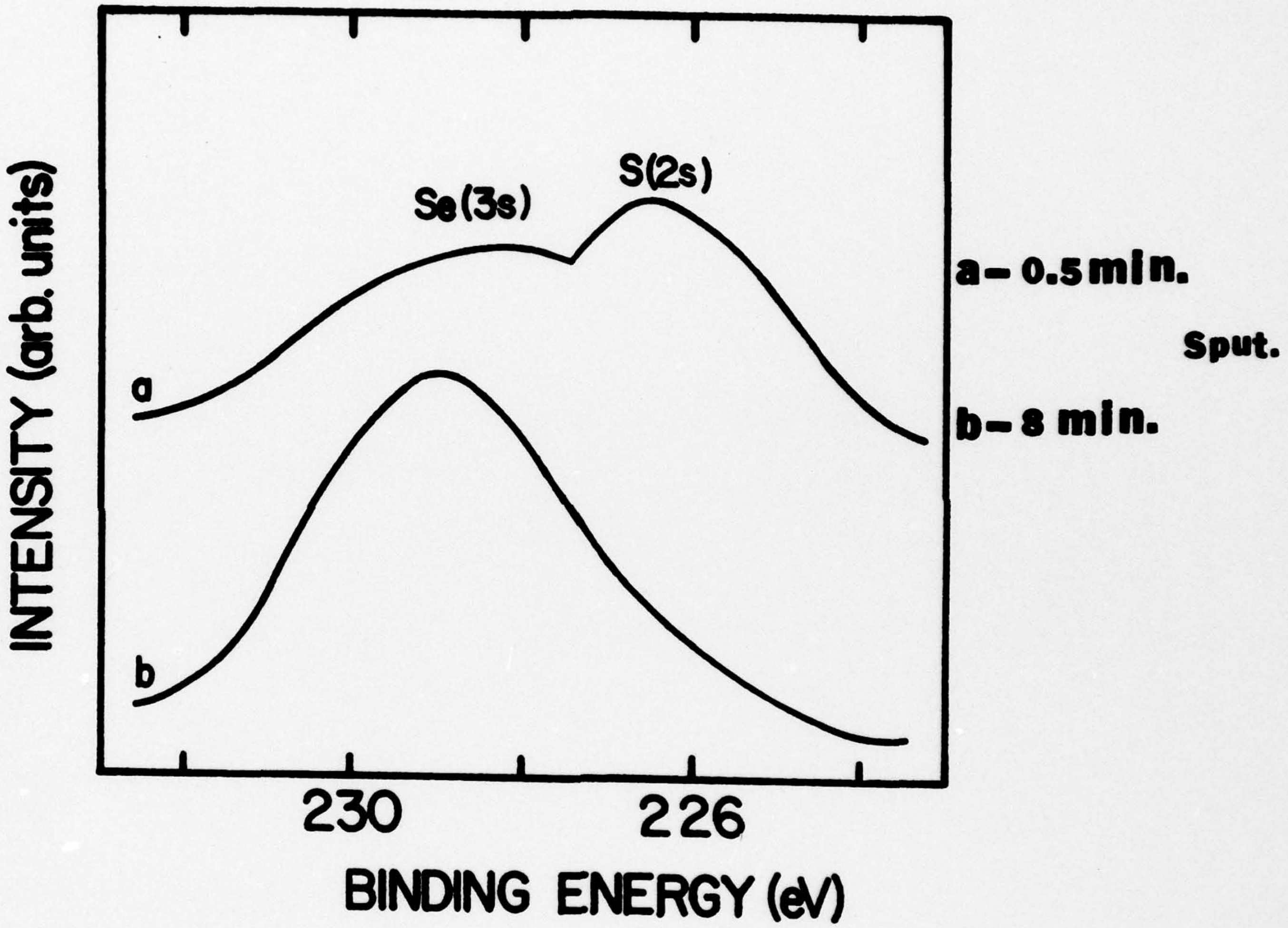

INTENSITY (arb. units)
Se(3s)
S(2s)
a
b
230
226
BINDING ENERGY (eV)
a– 0.5 min.
Sput.
b– 8 min.

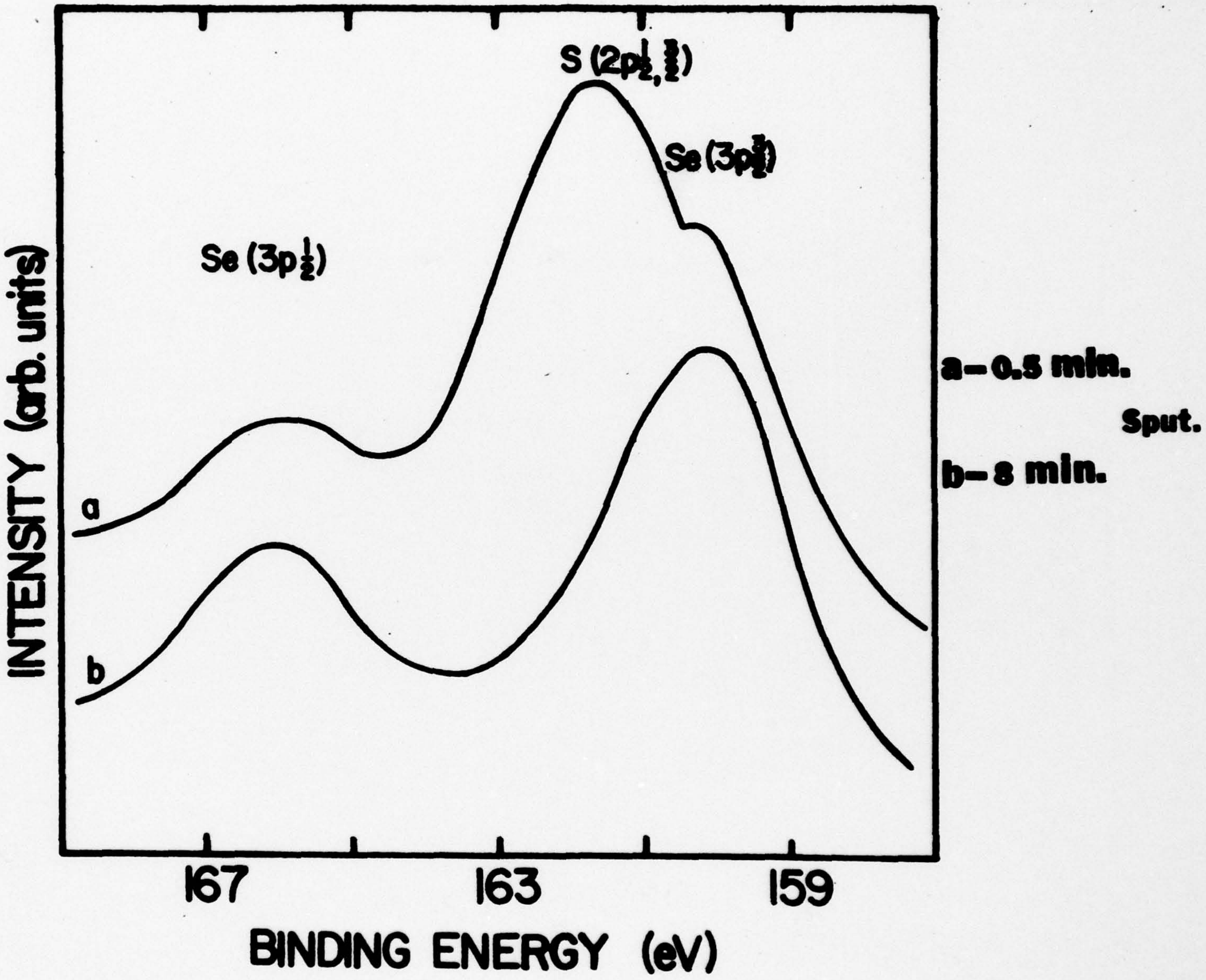
INTENSITY (arb. units)
BINDING ENERGY (eV)
167
163
159
Se (3p$\frac{1}{2}$)
S (2p$\frac{1}{2}$,$\frac{3}{2}$)
Se (3p$\frac{3}{2}$)
a
b
a– 0.5 min.
Sput.
b– 8 min.

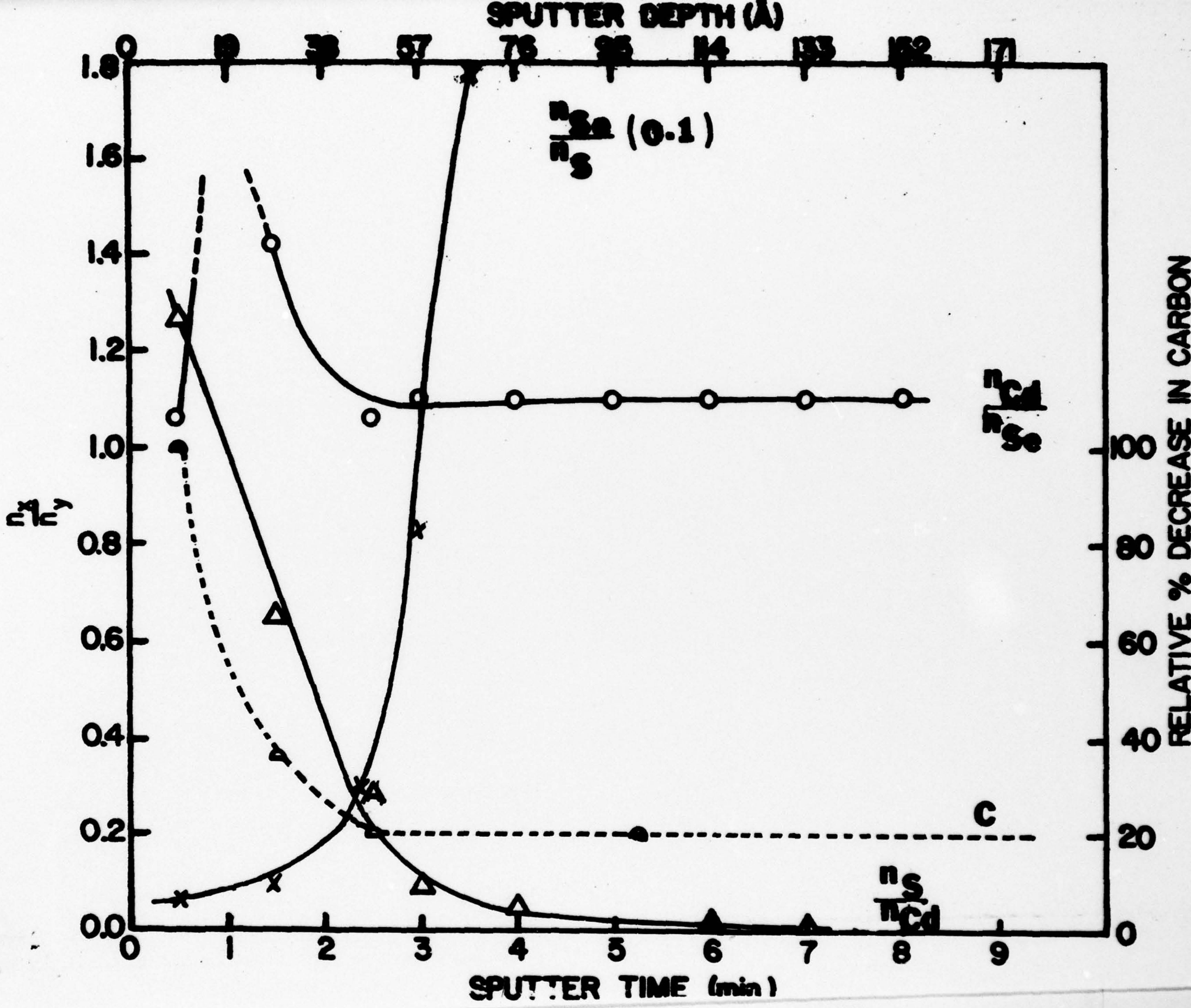
SPUTTER DEPTH (Å)
0
19
38
57
76
95
114
133
152
171
$\frac{n_{Se}}{n_S}$ (0.1)
$\frac{n_{Cd}}{n_{Se}}$
C
$\frac{n_S}{n_{Cd}}$
$\frac{n_x}{n_y}$
1.8
1.6
1.4
1.2
1.0
0.8
0.6
0.4
0.2
0.0
0
1
2
3
4
5
6
7
8
9
SPUTTER TIME (min)
RELATIVE % DECREASE IN CARBON
100
80
60
40
20
0

Fig 4

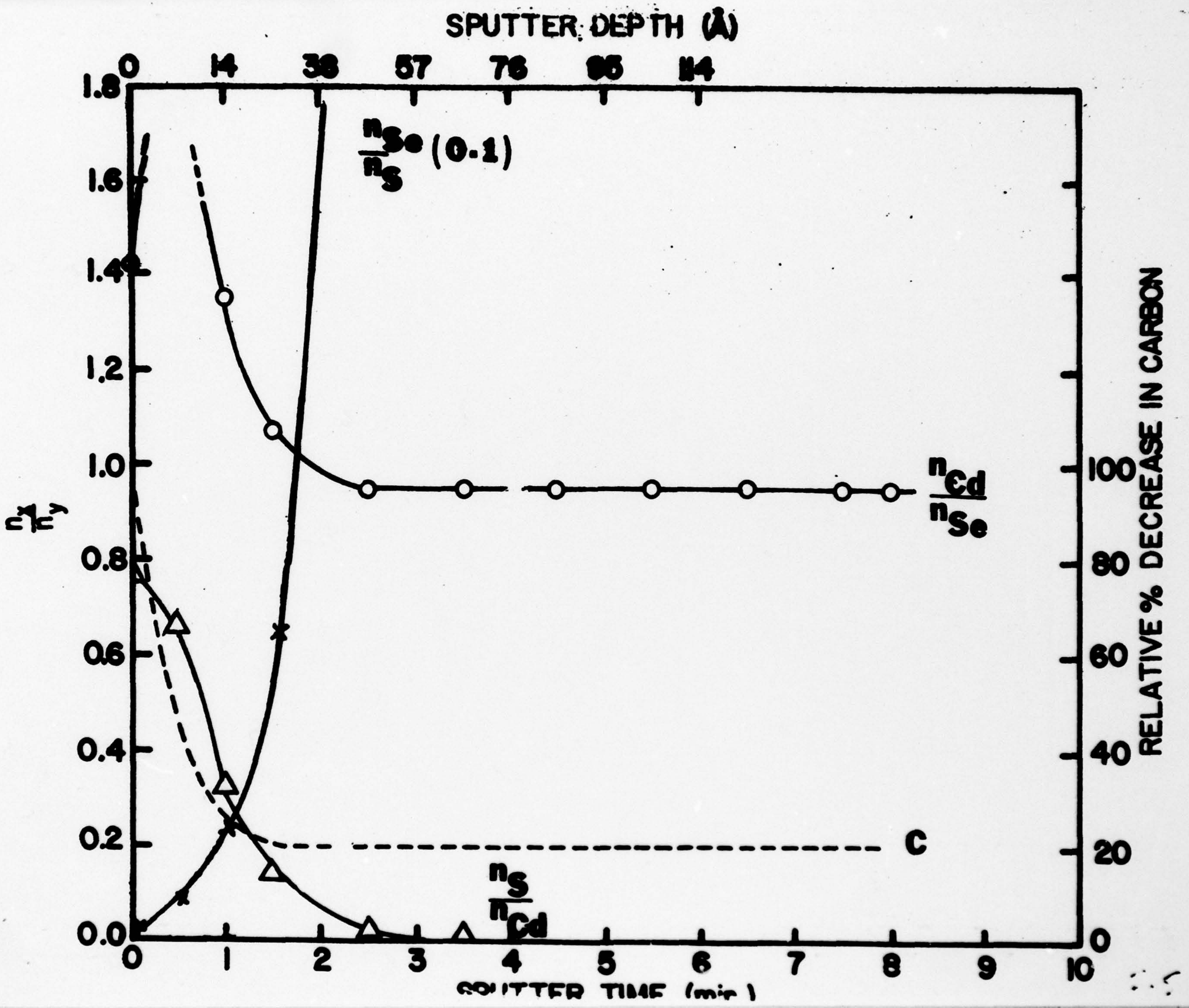
SPUTTER DEPTH (Å)
0
19
38
57
76
95
114
$\frac{n_x}{n_y}$
1.8
1.6
1.4
1.2
1.0
0.8
0.6
0.4
0.2
0.0
$\frac{n_{Se}}{n_S}$ (0.1)
$\frac{n_{Cd}}{n_{Se}}$
C
$\frac{n_S}{n_{Cd}}$
0
1
2
3
4
5
6
7
8
9
10
SPUTTER TIME (min)
RELATIVE % DECREASE IN CARBON
100
80
60
40
20
0

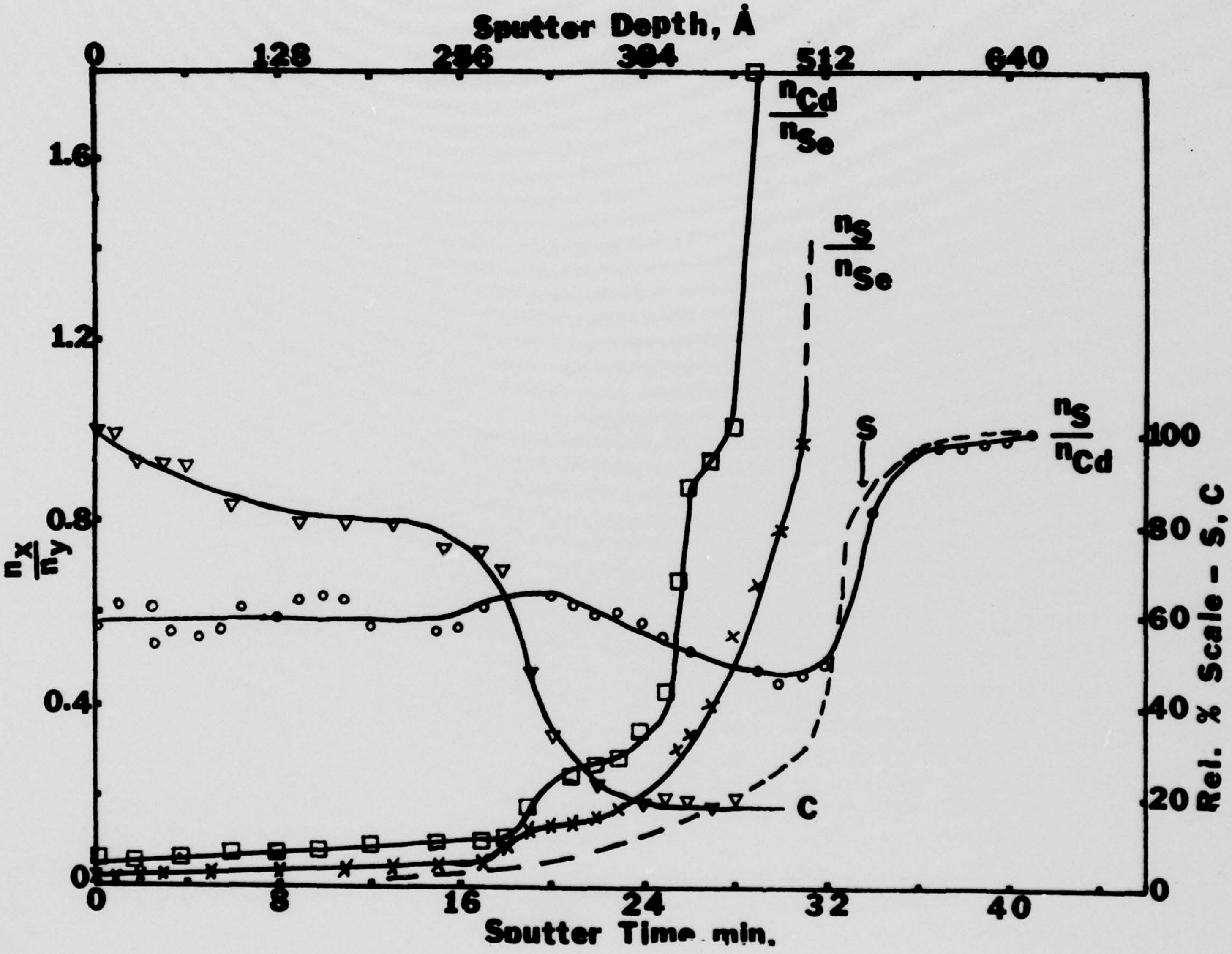
Sputter Depth, Å
0
128
256
384
512
640
$\frac{n_x}{n_y}$
0
0.4
0.8
1.2
1.6
Rel. % Scale – S, C
0
20
40
60
80
100
$\frac{n_{Cd}}{n_{Se}}$
$\frac{n_S}{n_{Se}}$
S
$\frac{n_S}{n_{Cd}}$
C
0
8
16
24
32
40
Sputter Time min.

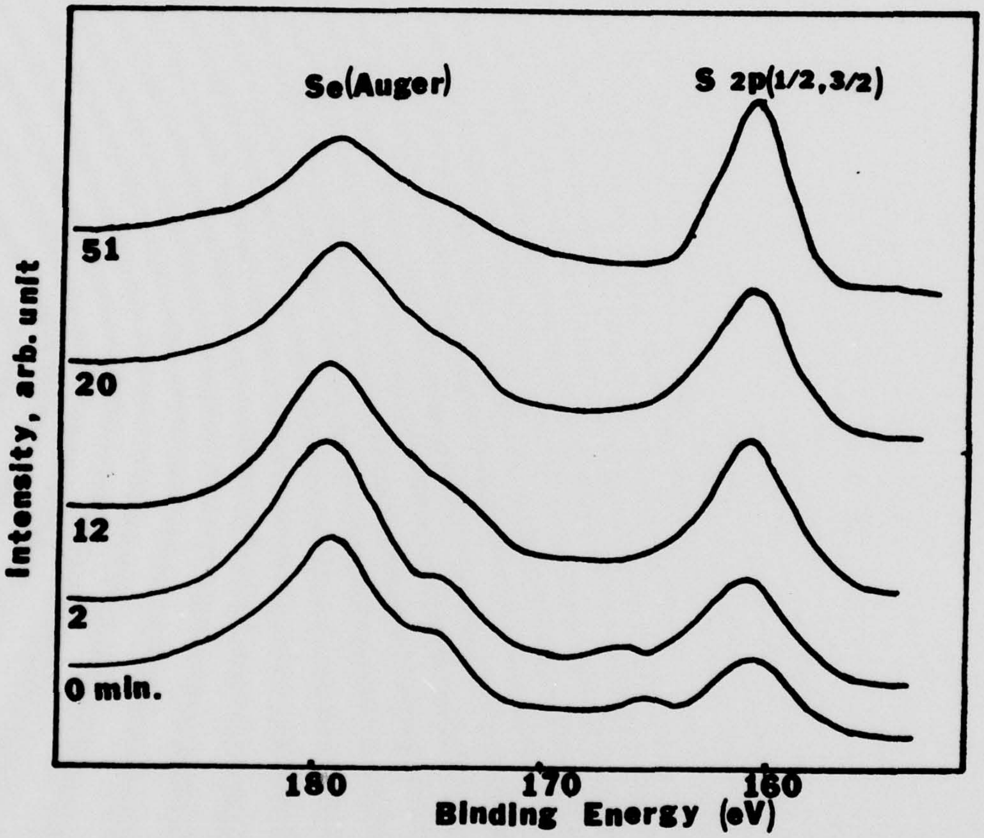
Se(Auger)
S 2p(1/2,3/2)
51
20
12
2
0 min.
Intensity, arb. unit
180
170
160
Binding Energy (eV)

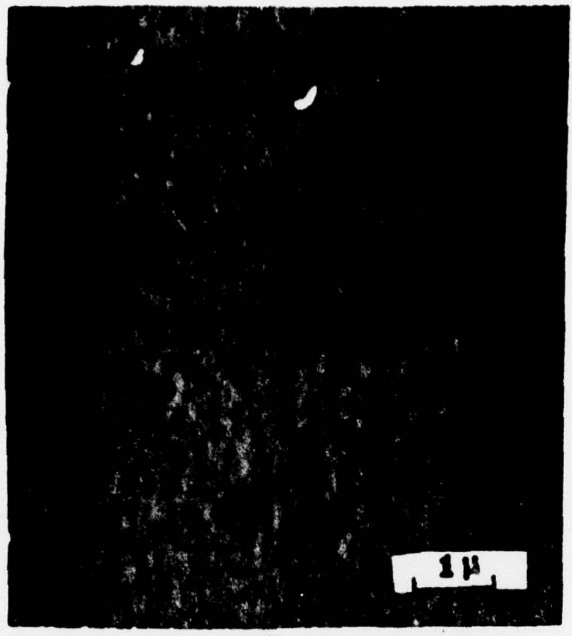

a

b

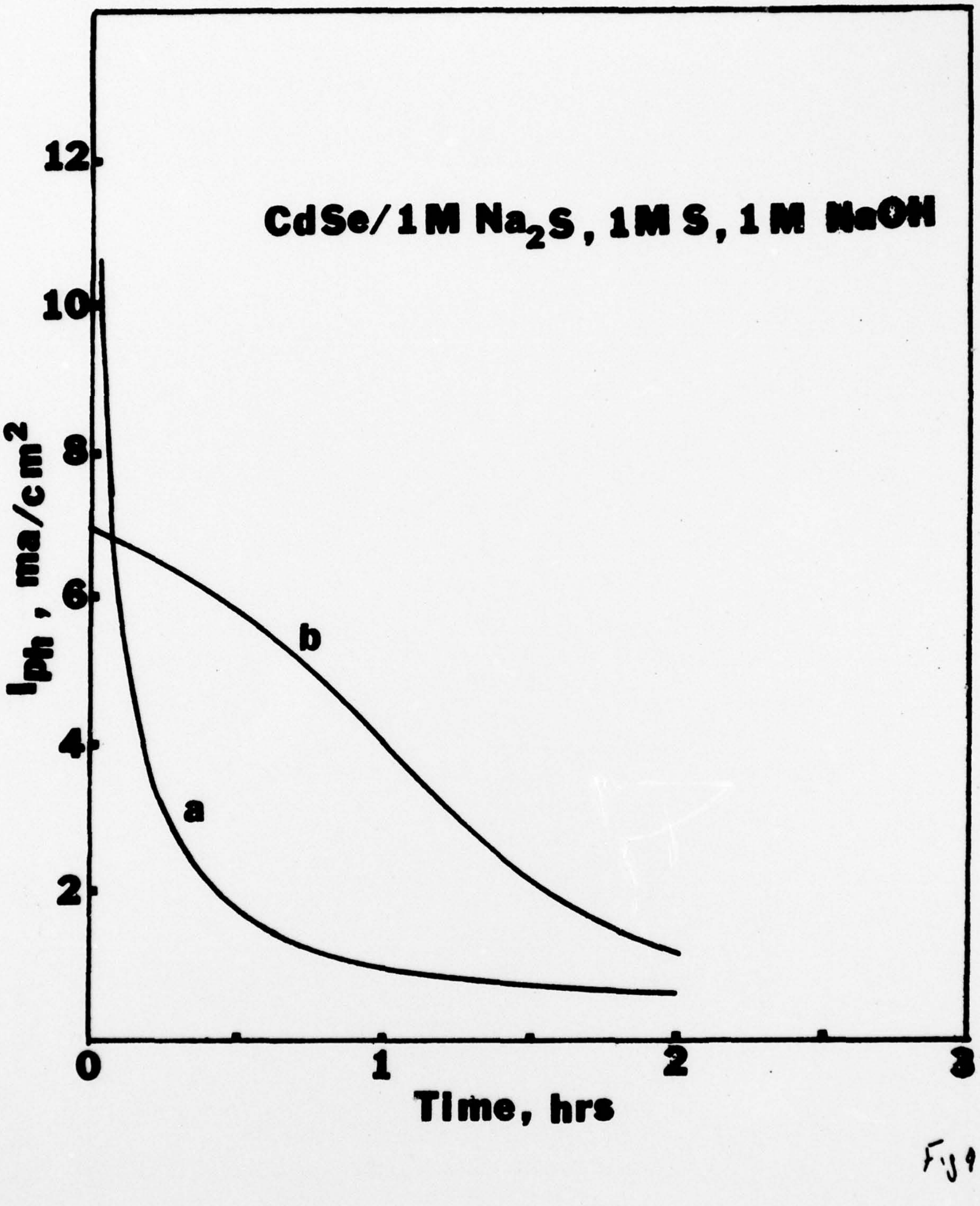

Fig 9

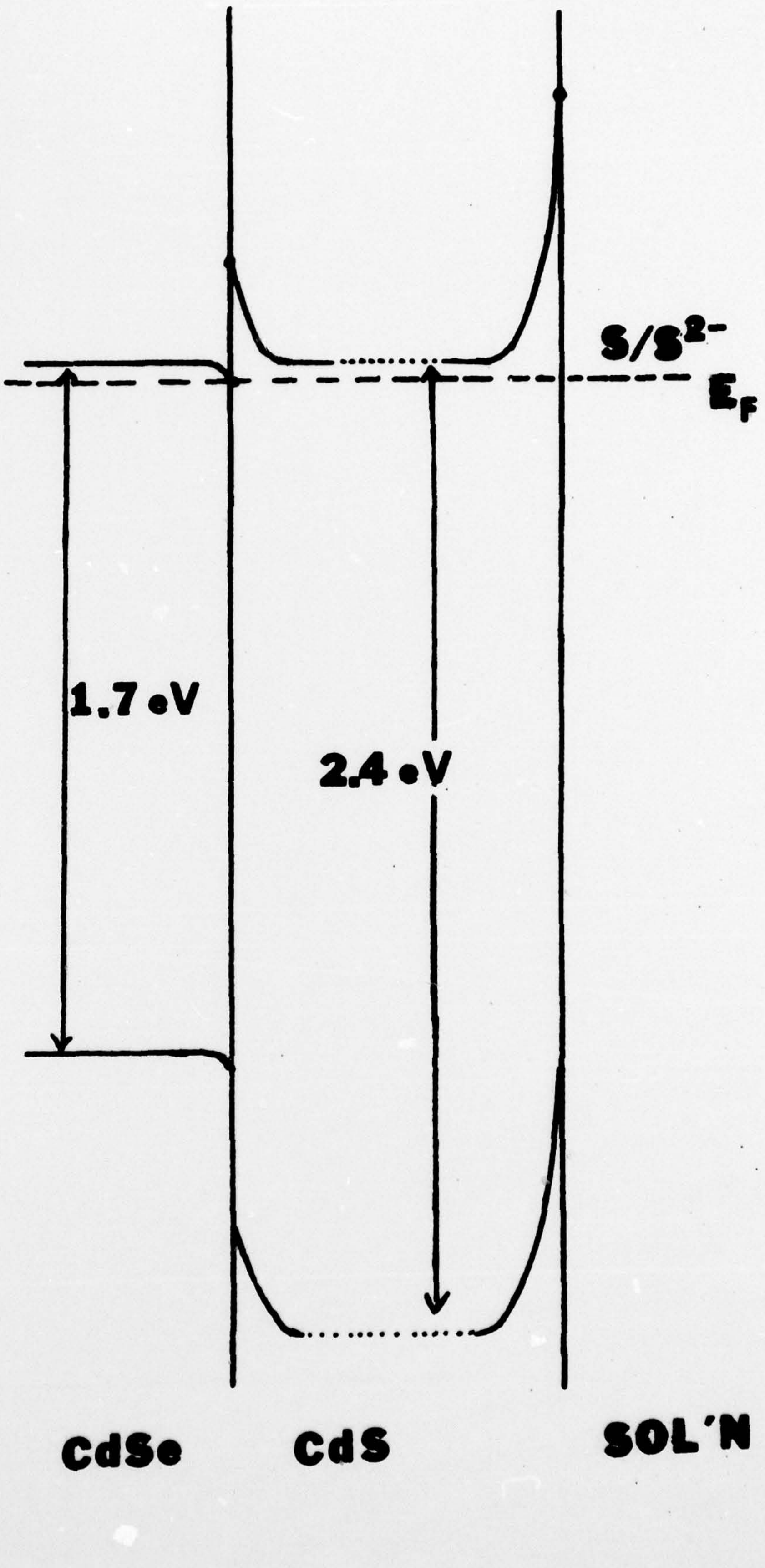

Fig 10

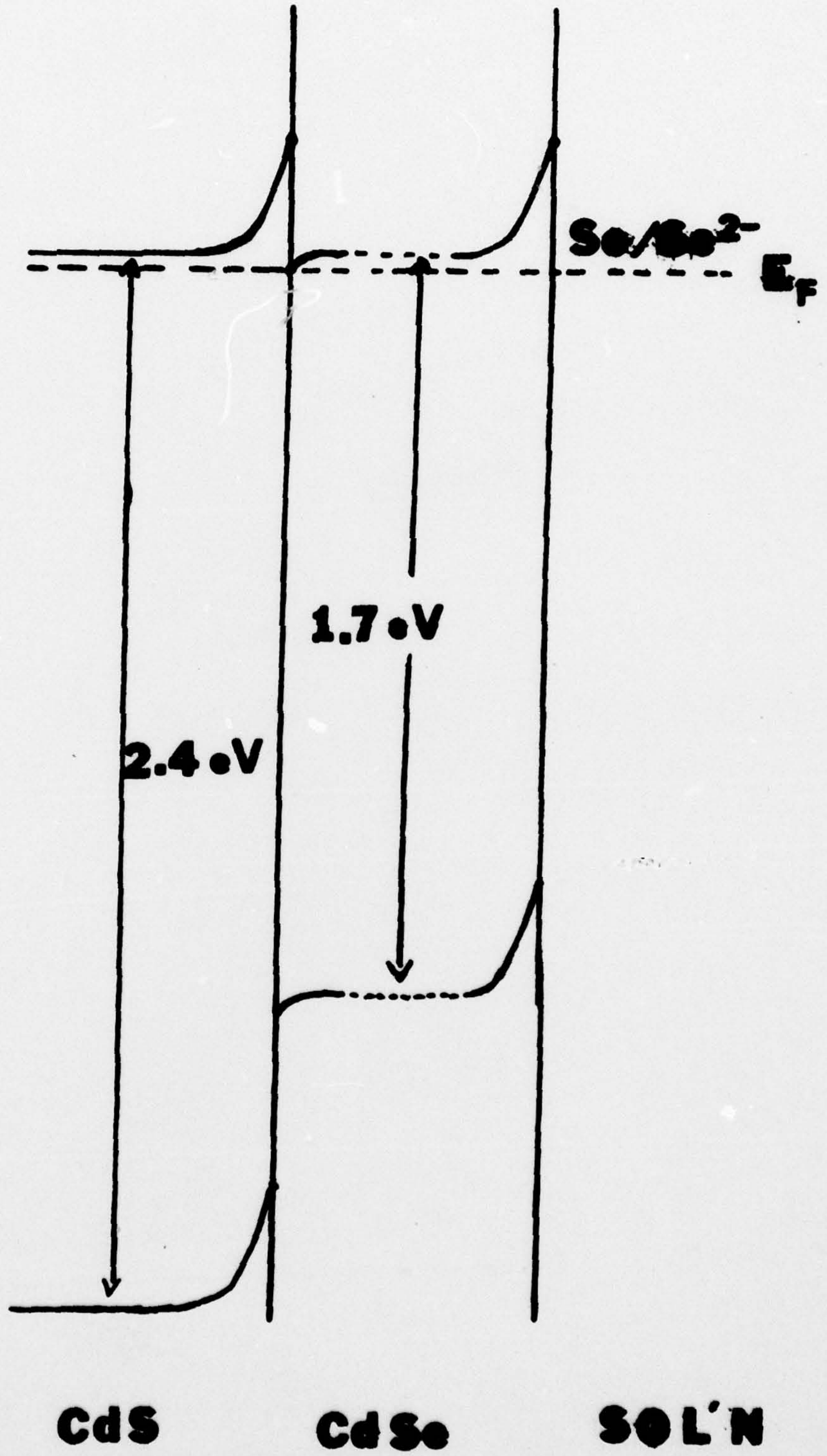

Fig 11